Robust Adaptive MMSE/DFE Multiuser Detection in Multipath Fading Channel with Impulse Noise

Bor-Sen Chen, *Fellow, IEEE*, Chang-Lan Tsai, and Chia-Sheng Hsu

***Abstract*—The direct-sequence code-division multiple-access (DS/CDMA) technique is extensively used for cellular, personal, and mobile radio communication systems. However, the conventional channel estimators cannot provide accurate channel information for multiuser detection in the presence of impulsive noise and Doppler spread, especially in the time-varying fading channel. We propose a linear-trend tracking method for estimating the impulse response of the time-varying channel via a robust Kalman filtering with a scheme that can automatically adjust the variance of the driving noise. The proposed method need not identify the parameters of the channel model and is insensitive to the speed of channel variation. Following channel estimation, a robust multiuser detection algorithm is developed via a Kalman-based decision feedback equalization (DFE). A nonlinear limitation function is incorporated to mitigate the effects of channel estimation error and impulsive noise and to prevent severe error propagation. Simulation results conclude that the performance of the DS/CDMA system is improved by using the proposed receiver.**

***Index Terms*—Channel estimation, CDMA, linear trend channel model, robust Kalman filtering.**

I. Introduction

DIRECT-SEQUENCE code-division multiple-access (DS/CDMA) communication systems are characterized by increased capacity in terms of the number of users per bandwidth unit, greater flexibility in the allocation of channels, light signaling protocols, the ability to operate asynchronously over multipath fading channels, as well as the capability of sharing bandwidth with narrowband communication systems [1], but DS/CDMA systems exhibit a capacity limit in the sense that there exists a maximum number of users that can simultaneously communicate over multipath fading channels for a specified level of performance per user. This limitation is caused by multiple-access interference (MAI) among the users and intersymbol interference (ISI) arising from the existence of different transmission paths.

The optimal multiuser detector [2], which minimizes the probability of bit error, is implemented by using the maximum likelihood (ML) sequence detection method via the Viterbi algorithm. However, the computational complexity of the Viterbi algorithm grows exponentially with the number of users and the length of the time-dispersive channel. Many suboptimal schemes have been studied to reduce the complexity. Linear filtering methods are explored in greater detail [3]–[9]. Channel estimation is required for coherent detection in most DS/CDMA receivers, including the Rake receiver, minimum-mean-square-error (MMSE) detectors [10], minimum variance detectors [11], and multistage interference cancellers [12]. Inaccurate channel estimates would lead to a large bit-error rate, especially with multiuser detection. Therefore, many joint channel estimation/symbol detection algorithms have been presented [7], [13], [14]. However, these channel estimators need to identify the channel coefficients, and channel noise is assumed to be Gaussian distributed.

It has been found that a variety of man-made noises (e.g., ignition noise, powerline noise, microwave oven noise), which are known to be major causes of errors in digital radio communications, are impulsive. Their statistical characteristics are very different from the Gaussian ones [15], [16]. Therefore, it is necessary to develop a robust receiver scheme for DS/CDMA in an impulsive noise channel. A robust multiuser detection technique has been developed to combat MAI and impulsive noise in CDMA communication systems in [15]. This technique employs the M-estimation method [22] for robust regression. Instead of minimizing a sum of squared residues, Wang and Poor minimized the sum of a less rapidly increasing function of the residues.

In this paper, the effects of both multipath time-varying fading and impulsive noise are considered in the design of a channel estimation and symbol detection algorithm for DS/CDMA systems. A robust linear-trend tracking algorithm and a robust multiuser detection algorithm are proposed to combat the multipath time-varying fading channel with impulsive noise. In contrast to the conventional autoregressive (AR) channel model [5], the proposed linear-trend channel model with a scheme for tuning the variance of the driving noise is less sensitive to channel variation due to the changing of Doppler frequency (for example, due to the changing of mobile speed). We need not identify the coefficients of the transition matrix of the linear-trend model. The time-varying fading channels are estimated by the proposed robust channel estimator with a self-tuning scheme to track the time-varying fading. Moreover, a decision feedback-based robust multiuser detection algorithm is derived by taking into consideration the channel estimation error. Nonlinear limitation functions are embedded into the robust channel estimator and robust multiuser detector to mitigate the impulsive noise. Finally, computer simulations are

Manuscript received May 17, 2002; revised December 22, 2003. This work was supported by National Science Council under Contract NSC 92-2213-E-007-083. The associate editor coordinating the review of this manuscript and approving it for publication was Prof. Xiaodong Wang.

B.-S. Chen and C.-L. Tsai are with the Department of Electrical Engineering, National Tsing Hua University, Hsinchu, Taiwan 30055, R.O.C. (e-mail: bschen@moti.ee.nthu.edu.tw).

C.-S. Hsu is with the Department of Algorithm Development, Sunplus Technology Co., Ltd., Hsinchu, Taiwan 300, R.O.C. (e-mail: pandahsu@sunplus.com.tw).

Digital Object Identifier 10.1109/TSP.2004.838949

given for comparison with other methods and to demonstrate the superiority of the proposed method.

The rest of this paper is organized as follows. Section II describes the channel model and presents the DS/CDMA transmitter and receiver structures. Section III proposes the linear-trend model for channel estimation. Section IV explains how the channel can be tracked in a time-varying Doppler environment. A self-tuning scheme is applied to automatically adjust the variance of the driving noise of the linear-trend model in the time-varying Doppler environment. The robust multiuser detector is illustrated in Section V. The bit-error rate performance of the robust multiuser detector is also simulated. Concluding remarks are finally made in Section VI.

II. Communication System Model

Consider a K-user binary DS/CDMA system. The transmitted signal due to the kth user is given by

$$s_k(t) = \sum_{n=0}^{\infty} b_k(n) \sum_{m=0}^{N-1} c_k(m)\varphi(t - mT_c - nT_b) \quad (1)$$

where $b_k(n)$ denotes the nth binary symbol of the kth user, T_b is the symbol period, and $\varphi(t)$ is the normalized chip waveform with finite duration $T_c = T_b/N$, i.e., $\varphi(t) = 0$ for $t \notin [0, T_c]$, and has energy $(1/N)$. The sequence $\{c_k(m)$, for $m = 0, 1, \ldots, N-1\}$, where N denotes the spreading factor, is a signature sequence of ± 1 assigned to the kth user. Due to the wideband signaling of DS/CDMA systems, the frequency-selective fading channel that distorts transmission is encountered in most situations. The complex baseband received signal due to the kth user is

$$\begin{aligned} y_k^c(t) &= \sum_{j=0}^{L_k-1} A_{k,j}(t) s_k(t - \tau_{k,j}) \\ &= \sum_{n=0}^{\infty} \sum_{m=0}^{N-1} b_k(n) c_k(m) g_k(t, t - (m + nN)T_c) \end{aligned} \quad (2)$$

where $g_k(t,\tau) = \sum_{j=0}^{L_k-1} A_{k,j}(t)\varphi(\tau - \tau_{k,j})$; $\tau_{k,j}$ is the time delay for the jth path of the k th user; $A_{k,j}(t)$ represents the complex amplitude attenuation factor of the kth user for the fading channel on the jth path; and L_k is the number of received replicas due to the kth user's signal. Assume that $g_k(t,\tau)$, for $k = 1, 2, \ldots, K$, has finite support of length LT_c, i.e., $g_k(t,\tau) = 0$ for $\tau \notin [0, \mathrm{LT}_c]$, for all t, for $k = 1, 2, \ldots, K$.

The received signal is the superposition of all signals from K users plus background noise. The received signal is

$$r^c(t) = \sum_{k=1}^{K} y_k^c(t) + w^c(t)$$

where $w^c(t)$ is the additive channel noise. At the receiver end, the received signal is first filtered by a chip-matched filter and then sampled at the chip rate to produce the discrete-time sequence [17]

$$r(i) = \int_{iT_c}^{(i+1)T_c} r^c(t)\varphi(t - iT_c)dt = \sum_{k=1}^{K} y_k(i) + w(i) \quad (3)$$

where

$$\begin{aligned} y_k(i) &= \sum_{j=0}^{L-1} h_k(i,j) b_k\left(\left\lfloor \frac{i-j}{N} \right\rfloor\right) c_k((i-j)_N) \\ w(i) &= \int_{iT_c}^{(i+1)T_c} w^c(t)\varphi(t - iT_c)\, dt \\ h_k(i,j) &= \int_0^{T_c} g_k(t + iT_c, t + jT_c)\varphi(t)\, dt. \end{aligned} \quad (4)$$

Here, $\lfloor i \rfloor$ denotes the largest integer smaller than or equal to i, and $(i)_N$ denotes "$i \bmod N$."

III. Channel Estimation with Linear-Trend Tracking Technique

A linear-trend channel model and a Kalman filtering algorithm are proposed for channel tracking. Here, we assume that $h_k(i,j)$ in (4) is invariant during a symbol interval, i.e., assume that the channel is slowly fading. Denoting the channel parameter in the nth symbol interval as $h_{k,j}(n)$, then $y_k(i)$ is expressed as

$$y_k(nN + i) = \sum_{j=0}^{L-1} h_{k,j}(n) b_k\left(n + \left\lfloor \frac{i-j}{N} \right\rfloor\right) c_k((i-j)_N)$$

for $i = 0, 1, \ldots, N-1$.

In the conventional state-space model of Rayleigh fading channel, the state-space model employs either the AR(1) or AR(2) process. In the AR(2) case, the channel model can be written as [5]

$$\begin{aligned} h_{k,j}(n) = -a_{k,j}(1)h_{k,j}(n-1) - a_{k,j}(2) \\ \cdot h_{k,j}(n-2) + z_{k,j}(n) \end{aligned} \quad (5)$$

where

$$a_{k,j}(1) = -2r_d \cos(2\pi\sqrt{2} f_d T_b), \quad a_{k,j}(2) = r_d^2 \quad (6)$$

and $z_{k,j}(n)$ is a complex zero mean white Gaussian process with variance $\sigma_{k,j}^2$. The parameter f_d is the Doppler frequency of the underlying fading channel, and r_d is the pole radius that corresponds to the steepness of the peaks of the power spectrum. At least three parameters (r_d, f_d, and $\sigma_{k,j}^2$, or equivalently $a_{k,j}(1), a_{k,j}(2)$, and $\sigma_{k,j}^2$) must be estimated before constructing the AR(2) state-space model. If the fading channel is stationary (i.e., $a_{k,j}(1), a_{k,j}(2)$, and $\sigma_{k,j}^2$ are constant), AR(2) is an adequate channel model when $a_{k,j}(1), a_{k,j}(2)$, and $\sigma_{k,j}^2$ are known. However, the signals are always transmitted over a variable environment (for example, the velocity of mobile changes). In this situation, the parameters $a_{k,j}(1), a_{k,j}(2)$,

and $\sigma^2_{k,j}$ should be time-varying, and real-time estimation of the parameters $a_{k,j}(1), a_{k,j}(2)$, and $\sigma^2_{k,j}$ in (5) may become difficult in practical applications.

Furthermore, channel estimation is very sensitive to the perturbations (errors) of a_1 and a_2 because they influence the location of the poles of the transfer function of the AR(2) model, especially when the poles are close to the unit circle [18]. Therefore, the AR(2) model is not suitable for the time-varying fading channel.

In this situation, a simple channel model, i.e., linear-trend channel model, is proposed for efficient channel estimation in the time-varying channel case from the perspective of the nonstationary time series forecast.

A. Linear-Trend (LT) Channel Model

The linear-trend (LT) model has been a simple and efficient way for local real-time forecasting of nonstationary time series [19]. This makes the LT model suitable for real-time channel estimation. The m step-ahead prediction of the jth channel path of the kth user is decomposed into three components: i) a local linear trend, ii) a local trend slope multiplied by m steps, and iii) a randomly varying modeling error. For a time-varying fading channel depicted in Fig. 1, we may model the channel variation as

$$h_{k,j}(n+m) = h_{k,j}(n) + m \cdot \eta_{k,j}(n) + v_{k,j}(n) \tag{7}$$

where $h_{k,j}(n)$ denotes the local linear trend component at time n, $\eta_{k,j}(n)$ denotes the "trend slope," and $v_{k,j}(n)$ denotes the modeling error, which is assumed to be a white random process with zero mean and variance $\sigma^2_{v_{k,j}}$. For the one step-ahead prediction case, i.e., $m = 1$, (7) can be reduced to

$$h_{k,j}(n+1) = h_{k,j}(n) + \eta_{k,j}(n) + v_{k,j}(n). \tag{8}$$

Since the trend slope $\eta_{k,j}(n)$ is random in practical channel, we assume $\eta_{k,j}(n)$ to be a random walk model

$$\eta_{k,j}(n+1) = \eta_{k,j}(n) + u_{k,j}(n) \tag{9}$$

where $u_{k,j}(n)$ is called the differential slope at n. We model $u_{k,j}(n)$ as a white Gaussian random process with zero mean and variance $\sigma^2_{u_{k,j}}$ and assume that $u_{k,j}(n)$ is uncorrelated with $v_{k,j}(n)$.

Combining (8) and (9) yields the dynamic state-space model

$$\begin{bmatrix} \eta_{k,j}(n+1) \\ h_{k,j}(n+1) \end{bmatrix} = \begin{bmatrix} 1 & 0 \\ 1 & 1 \end{bmatrix} \begin{bmatrix} \eta_{k,j}(n) \\ h_{k,j}(n) \end{bmatrix} + \begin{bmatrix} u_{k,j}(n) \\ v_{k,j}(n) \end{bmatrix}. \tag{10}$$

Define a new state vector $\mathbf{x}_k(n) = [\eta_{k,0}(n), h_{k,0}(n), \eta_{k,1}(n), h_{k,1}(n), \ldots, \eta_{k,L-1}(n), h_{k,L-1}(n)]^T$. Then, the dynamics of the state equation can be expressed as

$$\mathbf{x}_k(n+1) = \mathbf{D}_1 \mathbf{x}_k(n) + \mathbf{u}_k(n) \tag{11}$$

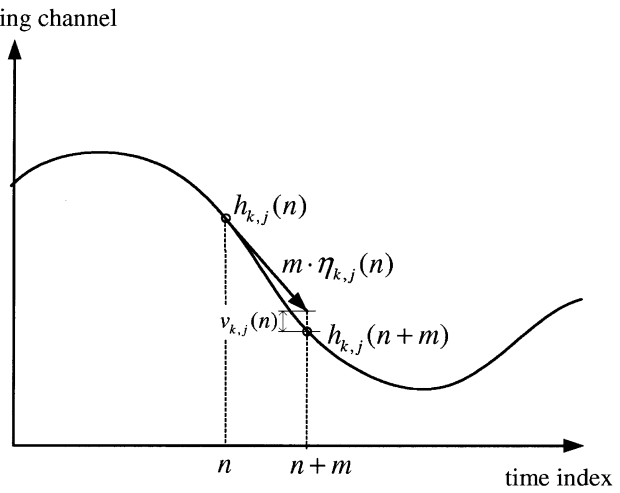

Fig. 1. Linear-trend channel model.

where we have the equation at the bottom of the page, where $\mathbf{I}_L$ denotes a $L \times L$ identity matrix, and the operator $\otimes$ denotes the Kronecker matrix product.

Stacking the K state vectors

$$\mathbf{x}(n) = \begin{bmatrix} \mathbf{x}_1^T(n) & \mathbf{x}_2^T(n) & \cdots & \mathbf{x}_K^T(n) \end{bmatrix}^T$$

the dynamics of the augmented state vector is expressed as

$$\mathbf{x}(n+1) = \mathbf{F}\mathbf{x}(n) + \mathbf{u}(n) \tag{12}$$

where

$$\mathbf{F} = \mathbf{I}_K \otimes \mathbf{D}_1$$
$$\mathbf{u}(n) = \begin{bmatrix} \mathbf{u}_1^T(n) & \mathbf{u}_2^T(n) & \cdots & \mathbf{u}_K^T(n) \end{bmatrix}^T.$$

Remark 1: In the channel model (11), the local linear trend and local trend slope are state variables for describing the dynamics of channel variation. Since the transition matrix $\mathbf{D}_1$ is fixed, we only need to estimate the variance of the driving noise. This simple model is very suitable for real-time estimation of the time-varying fading channel.

The variance of the driving noise $u_{k,j}(n)$ is determined by

$$\begin{aligned} \sigma^2_{u_{k,j}} &= E\{|u_{k,j}(n)|^2\} \\ &= E\{|\eta_{k,j}(n+1) - \eta_{k,j}(n)|^2\} \\ &= E\{|[h_{k,j}(n+2) - h_{k,j}(n+1) - v_{k,j}(n+1)] \\ &\quad - [h_{k,j}(n+1) - h_{k,j}(n) - v_{k,j}(n)]|^2\} \\ &= 6r_{h_{k,j}}(0) - 8r_{h_{k,j}}(1) + 2r_{h_{k,j}}(2) - 2\sigma^2_{v_{k,j}} \end{aligned} \tag{13}$$

where

$$r_{h_{k,j}}(m) = E\{h_{k,j}(n+m)h^*_{k,j}(n)\} = \sigma^2_{h_{k,j}} J_0(2\pi f_d m T_b)$$

in which the correlation function $r_{h_{k,j}}(m)$ of the channel coefficient $h_{k,j}(n)$ is defined by the zero-order Bessel function of the

$$\mathbf{D}_1 = \mathbf{I}_L \otimes \begin{bmatrix} 1 & 0 \\ 1 & 1 \end{bmatrix}$$
$$\mathbf{u}_k(n) = [u_{k,0}(n) \quad v_{k,0}(n) \quad u_{k,1}(n) \quad v_{k,1}(n) \quad \cdots \quad u_{k,L-1}(n) \quad v_{k,L-1}(n)]^T$$

first kind $J_0(\cdot)$ [6]. $\sigma^2_{h_{k,j}} = E\{|h_{k,j}(n)|^2\}$ denotes the power of the fading channel $h_{k,j}(n)$. However, when the Doppler frequency f_d is time-varying, it is difficult to estimate the actual f_d to upgrade the variance of the driving noise to fit with the fading channel. A self-tuning scheme based on the estimated slope will be employed to update the noise variance $\sigma^2_{u_{k,j}}$ and $\sigma^2_{v_{k,j}}$ to guarantee robust state estimation of (11). It will be discussed in detail later.

B. State-Space Signal Model

Because of the implicit upsampling within the spreading operation, a DS/CDMA system is a periodically time-varying transmission system and the received signal $r(i)$ is a cyclostationary process. The received signal $r(i)$ may be vectorized by stacking N consecutive elements in vector $\mathbf{r}(n)$, where n denotes the symbol index. Similarly, the channel output from the kth user can be written as

$$\begin{aligned}\mathbf{y}_k(n) &= [y_k(nN) \quad y_k(nN+1) \quad \cdots \quad y_k(nN+N-1)]^T \\ &= \mathbf{C}_k\mathbf{B}_k(n)\mathbf{h}_k(n) \end{aligned} \tag{14}$$

where we have the equations shown at the bottom of the page. The received signal $\mathbf{r}(n)$ is the sum of all users' signals and the additive channel noise

$$\begin{aligned}\mathbf{r}(n) &= [r(nN) \quad r(nN+1) \quad \cdots \quad r(nN+N-1)]^T \\ &= \mathbf{C}\mathbf{B}(n)\mathbf{h}(n) + \mathbf{w}(n) \end{aligned} \tag{15}$$

where

$$\begin{aligned}\mathbf{B}(n) &= \text{diag}(\mathbf{B}_1(n) \quad \mathbf{B}_2(n) \quad \cdots \quad \mathbf{B}_K(n)) \\ \mathbf{C} &= [\mathbf{C}_1 \quad \mathbf{C}_2 \quad \cdots \quad \mathbf{C}_K] \\ \mathbf{h}(n) &= \left[\mathbf{h}_1^T(n) \quad \mathbf{h}_2^T(n) \quad \cdots \quad \mathbf{h}_K^T(n)\right]^T \\ \mathbf{w}(n) &= [w(nN) \quad w(nN+1) \quad \cdots \quad w(nN+N-1)]^T. \end{aligned} \tag{16}$$

$\text{diag}(\mathbf{B}_1(n), \mathbf{B}_2(n), \ldots, \mathbf{B}_K(n))$ denotes a block diagonal matrix with diagonal submatrices $\mathbf{B}_1(n), \mathbf{B}_2(n), \ldots, \mathbf{B}_K(n)$.

The channel information $\mathbf{h}(n)$ can be obtained from the augmented state vector $\mathbf{x}(n)$

$$\mathbf{h}(n) = \mathbf{D}_h\mathbf{x}(n) \tag{17}$$

where $\mathbf{D}_h = \mathbf{I}_{KL} \otimes [0 \ 1]$. Therefore, the overall dynamics of the state equation can be expressed as

$$\begin{aligned}\mathbf{x}(n+1) &= \mathbf{F}\mathbf{x}(n) + \mathbf{u}(n) \\ \mathbf{r}(n) &= \mathbf{G}(n)\mathbf{x}(n) + \mathbf{w}(n) \end{aligned} \tag{18}$$

where $\mathbf{G}(n) = \mathbf{C}\mathbf{B}(n)\mathbf{D}_h$.

Remark 2: Although we have assumed that the spreading code is symbol-periodic, aperiodic spreading code can still be employed in our formulation after modifying the content of the matrix $\mathbf{C}_k$ in (16). In the case of aperiodic spreading codes, the matrix becomes a time-varying matrix $\mathbf{C}_k(n)$ because the spreading code changes from symbol to symbol.

In the next subsection, we will employ the Kalman filtering method to estimate the multipath fading channel with impulsive noise.

C. Recursive Channel Estimation

The Kalman filter is employed for the estimation of the state vector $\mathbf{x}(n)$ from the received signal $\mathbf{r}(n)$ such that the mean-square error (MSE) $E\{[\mathbf{x}(n) - \hat{\mathbf{x}}(n)]^H[\mathbf{x}(n) - \hat{\mathbf{x}}(n)]\}$ is minimized, where $\hat{\mathbf{x}}(n)$ is the estimate of $\mathbf{x}(n)$, and E denotes statistical expectation. According to the state-space model (18), the Kalman filter algorithm is given by [20]

$$\hat{\mathbf{x}}(n) = \mathbf{F}\hat{\mathbf{x}}(n-1) + \mathbf{K}_x(n)\mathbf{e}(n) \tag{19}$$

where $\mathbf{e}(n) = \mathbf{r}(n) - \mathbf{G}(n)\mathbf{F}\hat{\mathbf{x}}(n-1)$ denotes the innovation process, and $\mathbf{K}_x(n)$ is the Kalman gain. The initial state $\hat{\mathbf{x}}(0)$ is defined as a zero vector. The filter gain and error covariance matrices are obtained from the following recursive equations:

$$\mathbf{P}_{n\,|\,n-1} = \mathbf{F}\mathbf{P}_{n-1}\mathbf{F}^H + \mathbf{Q}_u \tag{20}$$

$$\mathbf{K}_x(n) = \mathbf{P}_{n\,|\,n-1}\mathbf{G}^H(n)[\mathbf{G}(n)\mathbf{P}_{n\,|\,n-1}\mathbf{G}^H(n) + \mathbf{Q}_w]^{-1} \tag{21}$$

$$\mathbf{P}_n = [\mathbf{I} - \mathbf{K}_x\mathbf{G}(n)]\mathbf{P}_{n\,|\,n-1} \tag{22}$$

where $\mathbf{Q}_w$ is defined as $E\{\mathbf{w}(n)\mathbf{w}^H(n)\}$, and $\mathbf{Q}_u$ is defined as $E\{\mathbf{u}(n)\mathbf{u}^H(n)\}$. For independent, identically distributed (i.i.d.) channel noise, $\mathbf{Q}_w$ is defined as $\sigma_w^2\mathbf{I}_N$, where $\sigma_w^2 = E\{|w(n)|^2\}$. In (20), $\mathbf{P}_{n\,|\,n-1} = E\{[\mathbf{x}(n) - \mathbf{F}\hat{\mathbf{x}}(n-1)][\mathbf{x}(n) - \mathbf{F}\hat{\mathbf{x}}(n-1)]^H\}$ is the covariance matrix of state-prediction error $\mathbf{x}(n) - \mathbf{F}\hat{\mathbf{x}}(n-1)$,

---

$$\mathbf{C}_k = \begin{bmatrix} c_k(0) & \cdots & 0 & 0 & c_k(N-1) & \cdots & c_k(N-L+1) \\ c_k(1) & \ddots & 0 & 0 & 0 & \ddots & \vdots \\ \vdots & \ddots & c_k(0) & \vdots & \vdots & & c_k(N-1) \\ & & c_k(1) & 0 & & & 0 \\ \vdots & & \vdots & \vdots & & & \vdots \\ c_k(N-1) & \cdots & c_k(N-L) & 0 & 0 & & 0 \end{bmatrix}$$

$$\mathbf{B}_k(n) = [b_k(n)\mathbf{I}_L \quad b_k(n-1)\mathbf{I}_L]^T$$

$$\mathbf{h}_k(n) = [h_{k,0}(n) \quad h_{k,1}(n) \quad \cdots \quad h_{k,L-1}(n)]^T.$$

and $\mathbf{P}_n = E\{[\mathbf{x}(n) - \hat{\mathbf{x}}(n)][\mathbf{x}(n) - \hat{\mathbf{x}}(n)]^H\}$ in (22) is the covariance matrix of state-estimation error $\mathbf{x}(n) - \hat{\mathbf{x}}(n)$.

The recursive algorithm requires the knowledge of all users' spreading sequence $\{c_k(m)$, for $m = 0, 1, \ldots, N-1\}$ and symbols $\{b_k(n), b_k(n-1)\}$, for $k = 1, 2, \ldots, K$. For the uplink multiuser detection scenario, the base station knows the spreading sequences of all active users. The symbols of all users can be obtained via training sequence in the training mode or decision feedback in the tracking mode, respectively. In the tracking mode, the output symbols from the decision device $\{\hat{b}_k(n), \hat{b}_k(n-1)\}$, for $k = 1, 2, \ldots, K$, are feedback to the Kalman filter to update the channel parameters $\{h_{k,j}(n)$, and $\eta_{k,j}(n)$, for $k = 1, 2, \ldots, K, j = 0, 1, \ldots, L-1\}$, which are the state variables. Then, one-step prediction of the channel impulse response $\mathbf{h}(n+1)$ is performed by

$$\begin{aligned}\hat{\mathbf{h}}(n+1) &= \left[\hat{\mathbf{h}}_1^T(n+1) \quad \hat{\mathbf{h}}_2^T(n+1) \quad \cdots \quad \hat{\mathbf{h}}_K^T(n+1)\right]^T \\ &= \mathbf{D}_h \mathbf{F} \hat{\mathbf{x}}(n). \end{aligned} \tag{23}$$

The predicted channel is employed to estimate the symbols $\{\hat{b}_k(n+1)$, for $k = 1, 2, \ldots, K\}$, in the multiuser detector, which will be introduced in Section V.

IV. Robust Improvement of the Linear-Trend Channel Model

In this section, based on extensive simulations, a self-tuning scheme is proposed to improve the performance of the proposed LT model-based channel estimation without knowledge of the variances of $u_{k,j}(n)$ and $v_{k,j}(n)$ in (10). The robustness of the estimation scheme is illustrated via simulation, which indicate the potential of the proposed LT model as an effective method for estimating the time-varying fading channels.

In the simulations, each user is assigned with a short Gold sequence with a processing gain of 15. The chip waveform is a rectangular pulse. Jakes model [21] is adopted for the fading channels, where parameters are adjusted to represent different mobile speeds (or different Doppler frequencies). The carrier frequency and symbol interval are $f_c = 1800$ MHz and $T_b = 15.625$ μs, respectively. The data is binary phase shift keying (BPSK) modulated. The number of channel paths is assumed to be $L = 3$ for all users, with path powers $\sigma^2_{h_{k,0}} = 1, \sigma^2_{h_{k,1}} = 0.7, \sigma^2_{h_{k,2}} = 0.85$, respectively, for all $k = 1, 2, \ldots, K$, to produce a frequency-selective fading channel. The number of active users is $K = 5$ in all simulations. We assume $\tau_{k,j} = jT_c$, for all k, for simplicity.

In order to illustrate the channel estimation performance of the proposed algorithm, the normalized mean-square error (NMSE) of channel estimation is defined as

$$\text{NMSE}_k = \frac{\sum_{j=0}^{L-1} E\{|h_{k,j}(n) - \hat{h}_{k,j}(n)|^2\}}{\sum_{j=0}^{L-1} E\{|h_{k,j}(n)|^2\}} \tag{24}$$

where NMSE_k denotes the normalized mean-square error of the kth user channel estimate. The signal-to-noise ratio (SNR) is defined as the ratio of one-bit received energy to channel noise variance, i.e.,

$$\text{MSE}_k = \frac{N \sum_{j=0}^{L-1} E\{|h_{k,j}(n)|^2\}}{\sigma_w^2} \tag{25}$$

where MSE_k denotes the SNR value of the kth user, and σ_w^2 denotes the variance of the channel noise $E\{|w(k)|^2\}$.

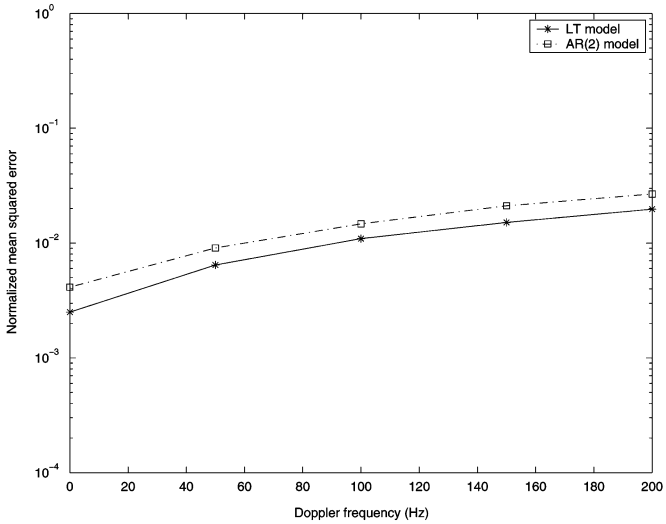

Fig. 2. Normalized mean-square error of channel estimation of user 1.

A. Channel Estimation for Different Doppler Frequencies

The simulated NMSE_1 values versus different Doppler frequencies 0, 50, 100, 150, and 200 Hz for the LT model and AR(2) model-based channel estimation are plotted in Fig. 2. We assume that all the paths have the same Doppler frequency. The parameters $a_{k,j}(1)$ and $a_{k,j}(2)$ for $k = 1, 2, \ldots, K, j = 0, 1, \ldots, L-1$ of the AR(2) model are defined by (6) according to the corresponding Doppler frequency. The variance $\sigma^2_{z_{k,j}}$ of the driving noise $z_{k,j}(n)$ in (5) is defined to satisfy the relation of a AR(2) process [20]

$$E\{|h_{k,j}(n)|^2\} = \left(\frac{1 + a_{k,j}(2)}{1 - a_{k,j}(2)}\right) \frac{\sigma^2_{z_{k,j}}}{[(1 + a_{k,j}(2))^2 - a^2_{k,j}(1)].} \tag{26}$$

For the LT channel model, the variance of the driving noise $u_{k,j}(n)$ is defined by (13), corresponding to different Doppler frequencies 0, 50, 100, 150, and 200 Hz, for all $k = 1, 2, \ldots, K, j = 0, 1, \ldots, L-1$.

Remark 3: The driving noise $u_{k,j}$ determines the variation of the channel trend $\eta_{k,j}(n)$. The variance $\sigma^2_{u_{k,j}}$ is not only governed by the Doppler frequency, as expressed in (13), but the variance of the additive noise. In the presence of channel noise, errors happen to the channel coefficient $h_{k,j}(n)$ and the trend $\eta_{k,j}(n)$. The variance $\sigma^2_{u_{k,j}}$ should be large enough to tune the next estimates back to the true values as possible. $\sigma^2_{u_{k,j}}$ is a compromise between the ideal value, which is defined in (13), and the noise variance.

The driving noise $v_{k,j}$ determines the variation of the channel coefficient $h_{k,j}(n)$. If the trend $\eta_{k,j}(n)$ is estimated precisely,

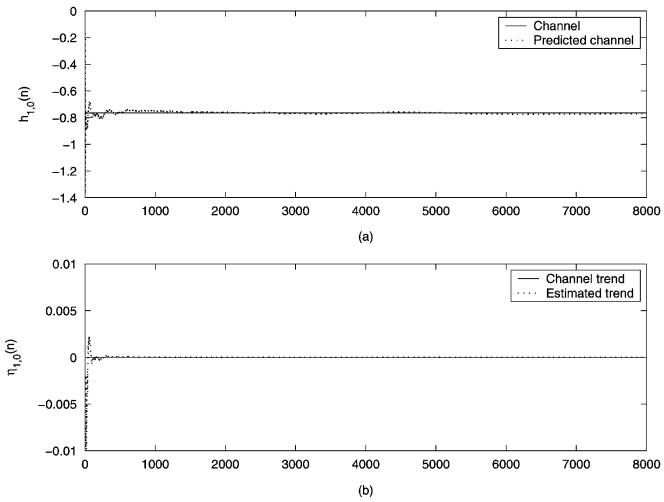

Fig. 3. (a) Real part of the predicted channel $\hat{h}_{1,0}(n)$ and actual channel impulse response $h_{1,0}(n)$. (b) Real part of the estimated trend $\hat{\eta}_{1,0}(n)$ and the actual channel trend $\eta_{1,0}(n) = h_{1,0}(n+1) - h_{1,0}(n)$ in the case of Doppler frequency 0 Hz.

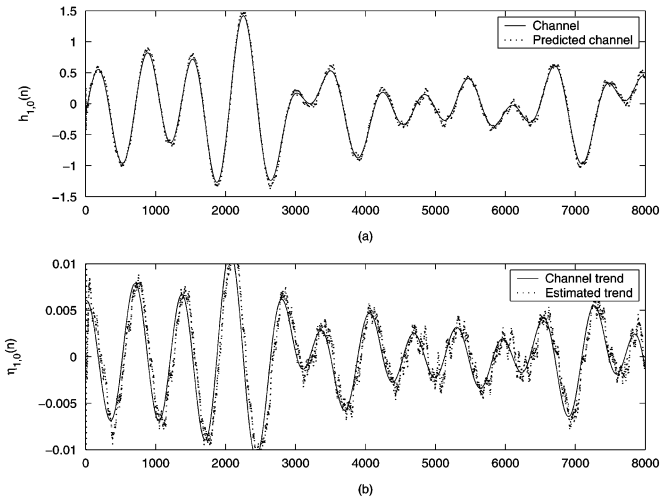

Fig. 4. (a) Real part of the predicted channel $\hat{h}_{1,0}(n)$ and actual channel impulse response $h_{1,0}(n)$. (b) Real part of the estimated trend $\hat{\eta}_{1,0}(n)$ and the actual channel trend $\eta_{1,0}(n) = h_{1,0}(n+1) - h_{1,0}(n)$ in the case of Doppler frequency 100 Hz.

the variance $\sigma^2_{v_{k,j}}$ is not critical to the performance. We can define $\sigma^2_{v_{k,j}}$ as a very small value.

In this simulation example, the SNR for each user is 12 dB. From Fig. 2, it is seen that the performance of the LT model is similar to that of the AR(2) model with exact knowledge of Doppler frequency, i.e., the exact Doppler frequency is used to defined the parameters $a_{k,j}(1), a_{k,j}(2)$, and $\sigma^2_{z_{k,j}}$. Defining the variance $\sigma^2_{v_{k,j}} = 0$, and $\sigma^2_{u_{k,j}}$ as 100 times the ideal values, which is clarified in (13), the LT model can track accurately the fading channel. Figs. 3–5 show the real parts of the predicted channel impulse response $\hat{h}_{1,0}(n)$ [shown in the subfigure (a)] obtained from (23), and channel trend $\hat{\eta}_{1,0}(n)$ [shown in the subfigure (b)] of the first path of user 1. The actual channel impulse response $h_{1,0}(n)$ and the channel trend $\eta_{1,0}(n) = h_{1,0}(n+1) - h_{1,0}(n)$ are also plotted. In Figs. 3–5, the Doppler frequencies are 0, 100, and 200 Hz, respectively. It is seen from the figures that the proposed algorithm can track accurately the channel impulse response and channel trend at different Doppler frequencies.

The variance of the driving noise $u_{k,j}(n)$, for all $k = 1, 2, \ldots, K, j = 0, 1, \ldots, L-1$, depends on the Doppler frequency according to (13). However, in practical wireless communications, the receiver cannot accurately know the Doppler frequency in each user's transmission channel. It is difficult to correctly determine the variances $\sigma^2_{u_{k,j}}$ of the LT model. A scheme to automatically adjust the variance of $u_{k,j}(n)$ is needed in the proposed LT model. Similar difficulties occur in determining the coefficients $a_{k,j}(1), a_{k,j}(2)$ and $\sigma^2_{k,j}$ of the AR(2) model in (5).

B. Scheme for Self-Tuning the Variance

For a fading channel with large Doppler frequency, the channel impulse response $h_{k,j}(n)$ changes rapidly. The variation of the channel trend $\eta_{k,j}(n) = h_{k,j}(n+1) - h_{k,j}(n)$ would be large. In this situation, we must set the variance $\sigma^2_{u_{k,j}}$ large. On the other hand, for a fading channel with small Doppler frequency, the channel impulse response changes mildly. The

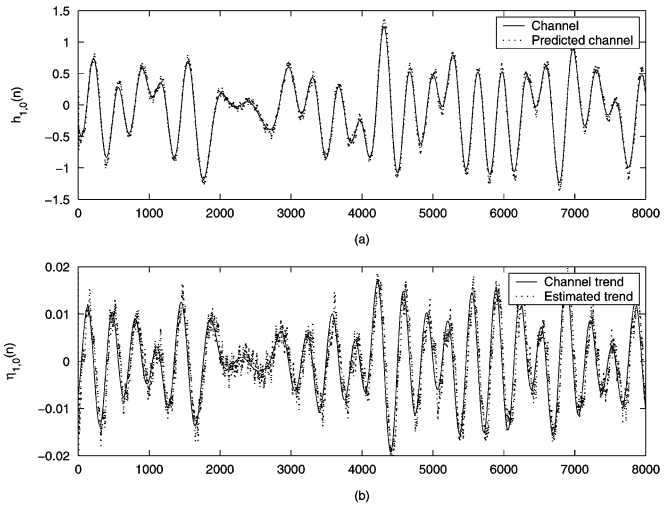

Fig. 5. (a) Real part of the predicted channel $\hat{h}_{1,0}(n)$ and actual channel impulse response $h1,0_(n)$. (b) Real part of the estimated trend $\hat{\eta}_{1,0}(n)$ and the actual channel trend $\eta_{1,0}(n) = h_{1,0}(n+1) - h_{1,0}(n)$ in the case of Doppler frequency 200 Hz.

variation of the channel trend would be small. We must set the variance of the driving noise small. The variances $\sigma^2_{u_{k,j}}$ and $\sigma^2_{v_{k,j}}$ can be adjusted according to the estimated local trend slope $\hat{\eta}_{k,j}(n)$. The variance self-tuning scheme is proposed as the following:

$$\hat{\sigma}^2_{u_{k,j}}(n+1) = \alpha|\hat{\eta}_{k,j}(n)| \tag{27}$$

$$\hat{\sigma}^2_{v_{k,j}}(n+1) = \beta|\hat{\eta}_{k,j}(n)| \tag{28}$$

where the positive constants α and β are chosen adequately to improve the performance.

Fig. 6 shows the NMSE_1 values versus SNR when the Doppler frequency of a fading channel varies from 50 to 100, 150, 200, 150, 100, 50, and 0 Hz, in proper sequence. All users are assumed to have the same SNR. The variance of the measurement noise $w(i)$ in (4) is determined by the specified SNR based on (25). The AR(2) model is assumed to know exactly the temporal

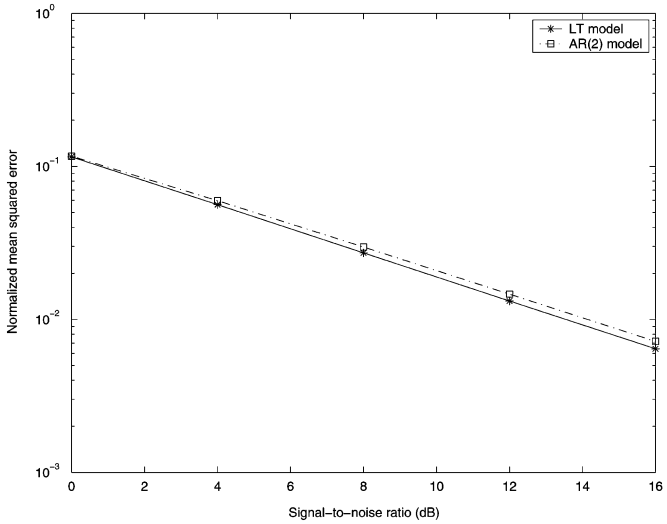

Fig. 6. Normalized mean-square error of channel estimation of user 1 for the channel with time-varying Doppler frequency versus SNR.

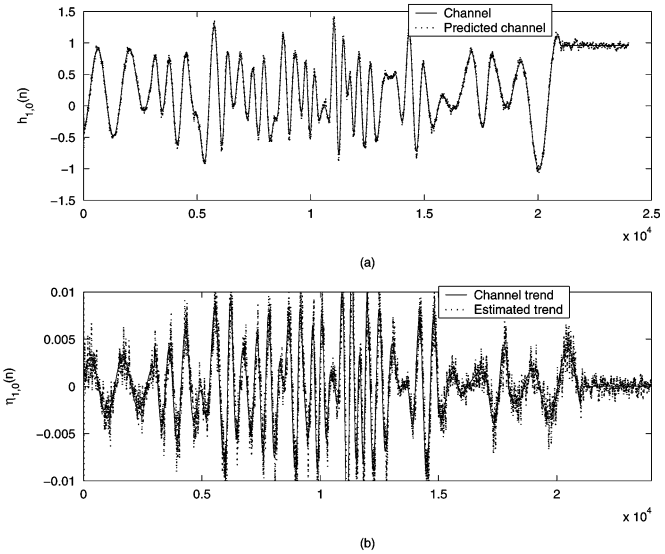

Fig. 7. (a) Real part of the predicted channel $\hat{h}_{1,0}(n)$ and actual channel impulse response $h_{1,0}(n)$. (b) Real part of the estimated trend $\hat{\eta}_{1,0}(n)$ and the actual channel trend $\eta_{1,0}(n) = h_{1,0}(n+1) - h_{1,0}$ in the channel with a time-varying Doppler frequency.

Doppler frequency to update the parameters $a_{k,j}(1), a_{k,j}(2)$, and $\sigma^2_{k,j}$ of the model in (5). In the recursive channel tracking based on the LT model, the automatic self-tuning rules in (27) and (28) are applied to adjust the variances $\sigma^2_{u_{k,j}}$ and $\sigma^2_{v_{k,j}}$, for $k = 1, 2, \ldots, K, j = 0, 1, \ldots, L-1$. The parameters α and β in (27) and (28) are specified as 1.5×10^{-4} and 0, respectively. The initial values of the variances are defined by $\sigma^2_{u_{k,j}}(1) = 1.5 \times 10^{-7}$ and $\sigma^2_{v_{k,j}}(1) = 0$. We can see that the accuracy of the LT model is slightly superior to that of the AR(2) model, which employs the accurate Doppler frequency to update the parameters exactly. Our proposed LT model combined with the self-tuning scheme can provide satisfactory performance in practical usage, where the Doppler frequency is not known.

The real parts of the predicted channel impulse response $\hat{h}_{1,0}(n)$ obtained from (23) and channel trend $\hat{\eta}_{1,0}(n)$ are plotted in Fig. 7(a) and (b), respectively. The MSE_1 is 12 dB. It is seen from Fig. 7 that the proposed algorithm can accurately track the channel impulse response and the channel trend when the Doppler frequency varies with time.

C. Robust Channel Estimation

When impulsive noise arises at the receiver, an impulsive component occurs in the innovation process $\mathbf{e}(n)$. In this situation, motivated by [15], we embed a nonlinear limiting function $\Omega_x(\cdot)$ into the Kalman filter to mitigate the effect of impulsive noise. A robust Kalman filter is proposed to treat this effect

$$\hat{\mathbf{x}}(n) = \mathbf{F}\hat{\mathbf{x}}(n-1) + \mathbf{K}_x \Omega_x(\mathbf{e}(n)) \tag{29}$$

where the output of the nonlinear limiting function $\Omega_x(\mathbf{e}(n))$ is a $N \times 1$ vector whose ith element is given by

$$\Omega_x(e_i(n)) = \begin{cases} e_i(n), & \text{if } |e_i(n)| \le \rho \\ \rho \cdot \text{sgn}(e_i(n)), & \text{otherwise.} \end{cases} \tag{30}$$

In (30), $\text{sgn}(\cdot)$ denotes the sign function; $e_i(n)$ is the ith entry of the complex vector $\mathbf{e}(n)$, for $i = 1, \ldots, N$; and ρ is the error threshold of the limiting function. The real and imaginary parts of $e_i(n)$ are treated independently. With a suitable choice of the error threshold ρ, the robust Kalman filter can reject the effects of impulsive noise and other interference and prevent error propagation due to the impulsive noise during channel estimation.

Remark 4: [15] Supposing that the additive channel noise is composed of two-term Gaussian mixture noise, the probability density function of the noise has the form

$$f = (1-\varepsilon)N(0, \nu^2) + \varepsilon N(0, \lambda\nu^2) \tag{31}$$

with $0 \le \varepsilon \le 1$ and $\lambda \ge 1$. Here, the $N(0, \nu^2)$ term represents the nominal noise, and the $N(0, \lambda\nu^2)$ term represents an impulsive component, with ε representing the probability that impulses occur. Then, we get the variance of additive noise as $\sigma_w^2 = (1-\varepsilon)\nu^2 + \varepsilon\lambda\nu^2$.

Fig. 8 illustrates the performance of channel estimation in the presence of non-Gaussian noise, which is generated by the two-term Gaussian mixture model depicted in (31) with parameters $\varepsilon = 0.1, \lambda = 10$, $\varepsilon = 0.01$, and $\lambda = 100$. The threshold ρ of the limiting function in the proposed robust LT-based Kalman filter in (29) is chosen as $1.5\sigma_w$. The total noise variance σ_w^2 can be easily estimated at the receiver. The time-varying channels simulated in Fig. 6 are used in this example. The results show that the robust estimators (with the aid of the limiting function $\Omega_x(\cdot)$, which can smooth the impulse-like noise) achieve better performance than the estimators without the limiting function, or equivalently, the threshold is defined as $\rho = \infty$. In the low SNR environment, the estimation $\hat{\eta}_{k,j}(n)$ is less accurate due to the large noise disturbance. The automatic variance tuning scheme's performance is inferior to the robust AR(2)-based Kalman filter model, which knows exactly the temporal Doppler frequency to update the coefficients. Nevertheless, when the SNR ratio is larger than 8 dB, the LT model with the variance self-tuning scheme can track the fading channel faithfully.

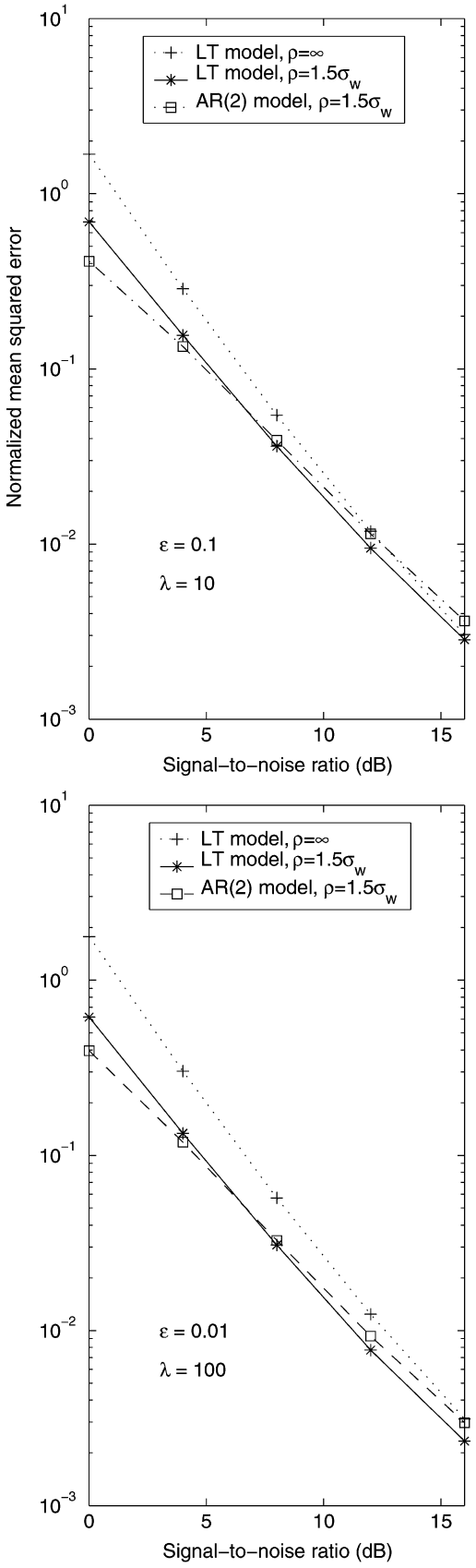

Fig. 8. Normalized mean-square error of channel estimation of user 1 for the channel with time-varying Doppler frequency disturbed by impulsive noise.

V. Adaptive MMSE/DFE Symbol Detection

In this section, a first-order linear state-space model is applied to the DS/CDMA system. Then, we can employ the Kalman filter to estimate simultaneously all users' symbols, which are embedded in the state vector, based on the predicted channel coefficients obtained via (23).

Define a state vector $\mathbf{b}(n) = [b_1(n), b_1(n-1), b_2(n), b_2(n-1), \ldots, b_K(n), b_K(n-1)]^T$, which contains the symbols contributing to the measurement $\mathbf{r}(n)$. The first-order (non-Gaussian) Markov transition model is defined by

$$\mathbf{b}(n+1) = \mathbf{A}\mathbf{b}(n) + \mathbf{v}(n+1) \tag{32}$$

where

$$\mathbf{A} = \mathbf{I}_K \otimes \begin{bmatrix} 0 & 0 \\ 1 & 0 \end{bmatrix}$$
$$\mathbf{v}(n) = [b_1(n) \quad 0 \quad b_2(n) \quad 0 \quad \cdots \quad b_K(n) \quad 0]^T.$$

The noise vector $\mathbf{v}(n)$ is white with zeros mean and covariance matrix

$$\mathbf{Q}_v = E\{\mathbf{v}(n)\mathbf{v}^H(n)\} = \mathbf{I}_K \otimes \begin{bmatrix} 1 & 0 \\ 0 & 0 \end{bmatrix}.$$

Next, we express (18) in the following form:

$$\mathbf{r}(n) = \mathbf{C}\mathbf{H}(n)\mathbf{b}(n) + \mathbf{w}(n) \tag{33}$$

where we have (34), shown at the bottom of the next page.

Since the transmitted symbols are embedded in the state vector $\mathbf{b}(n)$ in the transmission system (32) and (33), it is straightforward to employ the Kalman filter to estimate the desired state with the knowledge of the matrix $\mathbf{H}(n)$. However, only the channel predictions can be obtained. Re-express the received signal as

$$\mathbf{r}(n) = \mathbf{C}\hat{\mathbf{H}}(n)\mathbf{b}(n) + \mathbf{C}\tilde{\mathbf{H}}(n)\mathbf{b}(n) + \mathbf{w}(n) \tag{35}$$

where $\hat{\mathbf{H}}(n) = \text{diag}(\hat{\mathbf{h}}_1(n), \hat{\mathbf{h}}_1(n), \hat{\mathbf{h}}_2(n), \hat{\mathbf{h}}_2(n), \ldots, \hat{\mathbf{h}}_K(n), \hat{\mathbf{h}}_K(n))$ is composed of the predicted channel coefficients in (23), and $\tilde{\mathbf{H}}(n) = \mathbf{H}(n) - \hat{\mathbf{H}}(n)$ is the result of the prediction error. The disturbance resulting from channel prediction error $\mathbf{C}\tilde{\mathbf{H}}(n)\mathbf{b}(n)$ is uncorrelated with $\mathbf{C}\hat{\mathbf{H}}(n)\mathbf{b}(n)$. Therefore, it can be seen as random noise superimposed on $\mathbf{C}\hat{\mathbf{H}}(n)\mathbf{b}(n)$. Define the total noise contribution as

$$\mathbf{q}(n) = \mathbf{C}\tilde{\mathbf{H}}(n)\mathbf{b}(n) + \mathbf{w}(n) \tag{36}$$

which is with zero mean and covariance matrix $\mathbf{Q}(n) = \mathbf{Q}_w + \mathbf{C}E\{\tilde{\mathbf{H}}(n)\tilde{\mathbf{H}}^H(n)\}\mathbf{C}^H$. Therefore, the recursions of the Kalman filter for signal detection is

$$\mathbf{R}_{n\,|\,n-1} = \mathbf{A}\mathbf{R}_{n-1}\mathbf{A}^T + \mathbf{Q}_v \tag{37}$$
$$\mathbf{K}_b(n) = \mathbf{R}_{n\,|\,n-1}\hat{\mathbf{H}}^H(n)\mathbf{C}^H \times [\mathbf{C}\hat{\mathbf{H}}(n)\mathbf{R}_{n\,|\,n-1}\hat{\mathbf{H}}^H(n)\mathbf{C}^H + \mathbf{Q}(n)]^{-1} \tag{38}$$
$$\hat{\mathbf{b}}(n) = \mathbf{A}\hat{\mathbf{b}}(n-1) + \mathbf{K}_b(n) \times [\mathbf{r}(n) - \mathbf{C}\hat{\mathbf{H}}(n)\mathbf{A}\cdot \text{sgn}(\hat{\mathbf{b}}(n-1))] \tag{39}$$
$$\mathbf{R}_n = [\mathbf{I} - \mathbf{K}_b(n)\mathbf{C}\hat{\mathbf{H}}(n)]\mathbf{R}_{n\,|\,n-1} \tag{40}$$

where $\text{sgn}(\hat{\mathbf{b}}(n-1))$ represents the decision feedback operation. $\mathbf{R}_n$ and $\mathbf{R}_{n\,|\,n-1}$ denote the covariance matrices

of the estimation error $\mathbf{b}(n) - \hat{\mathbf{b}}(n)$ and prediction error $\mathbf{b}(n) - \mathbf{A}\hat{\mathbf{b}}(n-1)$, respectively.

Since the Kalman filter produces symbol estimates with the minimum mean-squared error (MMSE) among all linear filters, the recursive algorithm (37)–(40) is actually a MMSE/DFE algorithm, which simultaneously employs the decision-feedback equalization (DFE) technique and the MMSE approach. The *a priori* estimate $\mathbf{H}(n)\mathbf{A}\hat{\mathbf{b}}(n-1)$ are adopted to cancel ISI in $\mathbf{r}(n)$ via (39), and the decision outputs are fed back to the next state estimation.

In the above recursion, we need to compute the covariance matrix $E\{\tilde{\mathbf{H}}(n)\tilde{\mathbf{H}}^H(n)\}$. From the definition in (34), we have (41), shown at the bottom of the page, where $\tilde{\mathbf{h}}_k(n)$ is the channel prediction error $\mathbf{h}_k(n) - \hat{\mathbf{h}}_k(n)$. From (23), the predicted channel $\hat{\mathbf{h}}_k(n)$ is given by $\mathbf{D}_2\mathbf{D}_1\hat{\mathbf{x}}_k(n-1)$, where $\mathbf{D}_2$ is defined as $\mathbf{I}_L \otimes [0\ 1]$. If we partition the covariance matrix of the channel-prediction error $\mathbf{P}_{n|n-1}$ in (20) as

$$\mathbf{P}_{n|n-1} = \begin{bmatrix} \mathbf{P}_{n|n-1}^{(1,1)} & \mathbf{P}_{n|n-1}^{(1,2)} & \cdots & \mathbf{P}_{n|n-1}^{(1,K)} \\ \mathbf{P}_{n|n-1}^{(2,1)} & \mathbf{P}_{n|n-1}^{(2,2)} & & \mathbf{P}_{n|n-1}^{(2,K)} \\ \vdots & & \ddots & \\ \mathbf{P}_{n|n-1}^{(K,1)} & \mathbf{P}_{n|n-1}^{(K,2)} & & \mathbf{P}_{n|n-1}^{(K,K)} \end{bmatrix}$$

where each submatrix is with dimension $2L \times 2L$, then the covariance matrix of the channel-prediction error is

$$\begin{aligned} &E\left\{\tilde{\mathbf{h}}_k(n)\tilde{\mathbf{h}}_k^H(n)\right\} \\ &\quad = \mathbf{D}_2 E\{[\mathbf{x}_k(n) - \mathbf{D}_1\hat{\mathbf{x}}_k(n-1)] \\ &\qquad \times [\mathbf{x}_k(n) - \mathbf{D}_1\hat{\mathbf{x}}_k(n-1)]^H\}\mathbf{D}_2^H \\ &\quad = \mathbf{D}_2\mathbf{P}_{n|n-1}^{(k,k)}\mathbf{D}_2^H. \end{aligned}$$

A. Robust Symbol Detection

In (39), the residual signal $\tilde{\mathbf{r}}(n) = \mathbf{r}(n) - \mathbf{C}\hat{\mathbf{H}}(n)\mathbf{A} \cdot \mathrm{sgn}(\hat{\mathbf{b}}(n-1))$ is decomposed as

$$\begin{aligned} \tilde{\mathbf{r}}(n) = \sum_{k=1}^{K} &(\mathbf{C}_{k,1}\mathbf{h}_k(n)b_k(n) + \mathbf{C}_{k,2}\mathbf{h}_k(n)b_k(n-1) \\ &- \mathbf{C}_{k,2}\hat{\mathbf{h}}_k(n)\mathrm{sgn}(\hat{b}_k(n-1))) + \mathbf{w}(n) \end{aligned} \quad (42)$$

where $\mathbf{C}_{k,1}$ and $\mathbf{C}_{k,2}$ are the first L columns and the last L columns of the matrix $\mathbf{C}_k$, respectively. If the predicted channel $\hat{\mathbf{h}}_k(n)$ and the symbol estimation $\hat{b}_k(n-1)$, for all k, are correct, then the residual signal contains the desired signal component $\sum_{k=1}^{K}\mathbf{C}_{k,1}\mathbf{h}_k(n)b_k(n)$ and the additive white noise $\mathbf{w}(n)$. A limiting function can be applied to the residual signal to reject the interference and increase the accuracy of symbol estimation. The limiting function $\Omega_b(\tilde{\mathbf{r}}(n))$ is chosen as

$$\Omega_b(\tilde{r}_i(n)) = \begin{cases} \tilde{r}_i(n), & \text{if } |\tilde{r}_i(n)| \le \gamma \\ \gamma \cdot \mathrm{sgn}(\tilde{r}_i(n)), & \text{otherwise} \end{cases} \quad (43)$$

where $\tilde{r}_i(n)$ is the ith entry of the complex vector $\tilde{\mathbf{r}}(n)$, for $i = 0, 1, \ldots, N-1$. The real and imaginary parts of $\tilde{r}_i(n)$ are treated independently. The threshold γ must be determined carefully not to distort the desired signal component, i.e., γ should be greater than the absolute values of every components of the vector $\sum_{k=1}^{K}\mathbf{C}_{k,1}\mathbf{h}_k(n)b_k(n)$, and at the same time, it should be able to reject the interference as much as possible. Define $\mathbf{C}_{k,1}^{(i)}$ as the ith row of the matrix $\mathbf{C}_{k,1}$, for $i = 0, 1, \ldots, N-1$. The absolute value of $\tilde{r}_i(n)$ is upper bounded by

$$\begin{aligned} &\left|\sum_{k=1}^{K}\mathbf{C}_{k,1}^{(i)}\mathbf{h}_k(n)b_k(n)\right| \\ &\quad \le \sum_{k=1}^{K}\left|\mathbf{C}_{k,1}^{(i)}\mathbf{h}_k(n)b_k(n)\right| = \sum_{k=1}^{K}\left|\mathbf{C}_{k,1}^{(i)}\mathbf{h}_k(n)\right| \\ &\quad \le \sum_{k=1}^{K}\sum_{j=0}^{L-1}|h_{k,j}(n)|. \end{aligned} \quad (44)$$

Therefore, we can define the threshold $\gamma = \sum_{k=1}^{K}\sum_{j=0}^{L-1}|h_{k,j}(n)|$ for detecting the nth symbol of all users. The channel coefficients $h_{k,j}(n)$, for $k = 1, 2, \ldots, k, j = 0, 1, \ldots, L-1$, can be substituted by their predicted values in (23). Then, a robust symbol detection is

$$\begin{aligned} \hat{\mathbf{b}}(n) = \mathbf{A}\hat{\mathbf{b}}(n-1) + \mathbf{K}_b(n)\Omega_b(&\mathbf{r}(n) \\ &- \mathbf{C}\hat{\mathbf{H}}(n)\mathbf{A} \cdot \mathrm{sgn}(\hat{\mathbf{b}}(n-1))). \end{aligned} \quad (45)$$

instead of (39).

Assuming that the decision feedback symbols are correct, then the input to the limiting function is

$$\begin{aligned} \tilde{\mathbf{r}}(n) &= \sum_{k=1}^{K}\mathbf{C}_{k,1}\hat{\mathbf{h}}_k(n)b_k(n) + \sum_{k=1}^{K}\mathbf{C}_{k,1}\tilde{\mathbf{h}}_k(n)b_k(n) + \mathbf{w}(n) \\ &= \sum_{k=1}^{K}\mathbf{C}_{k,1}\hat{\mathbf{h}}_k(n)b_k(n) + \mathbf{q}(n) \end{aligned} \quad (46)$$

where $\mathbf{q}(n)$ is defined in (36). With the aid of the limiting function in (43), which can cut the large noise, from (35), (36), and (46), the output of the limiting function $\Omega_b(\tilde{\mathbf{r}}(n))$ is represented as

$$\Omega_b(\tilde{\mathbf{r}}(n)) = \sum_{k=1}^{K}\mathbf{C}_{k,1}\hat{\mathbf{h}}_k(n)b_k(n) + \mathbf{q}'(n) \quad (47)$$

$$\mathbf{H}(n) = \mathrm{diag}(\mathbf{h}_1(n) \quad \mathbf{h}_1(n) \quad \mathbf{h}_2(n) \quad \mathbf{h}_2(n) \quad \cdots \quad \mathbf{h}_K(n) \quad \mathbf{h}_K(n)). \quad (34)$$

$$\begin{aligned} E\{\tilde{\mathbf{H}}(n)\tilde{\mathbf{H}}^H(n)\} = \mathrm{diag}\Big(&E\left\{\tilde{\mathbf{h}}_1(n)\tilde{\mathbf{h}}_1^H(n)\right\} \quad E\left\{\tilde{\mathbf{h}}_1(n)\tilde{\mathbf{h}}_1^H(n)\right\} \quad E\left\{\tilde{\mathbf{h}}_2(n)\tilde{\mathbf{h}}_2^H(n)\right\} \quad E\left\{\tilde{\mathbf{h}}_2(n)\tilde{\mathbf{h}}_2^H(n)\right\} \\ &\cdots E\left\{\tilde{\mathbf{h}}_K(n)\tilde{\mathbf{h}}_K^H(n)\right\} \quad E\left\{\tilde{\mathbf{h}}_K(n)\tilde{\mathbf{h}}_K^H(n)\right\}\Big) \end{aligned} \quad (41)$$

where $\mathbf{q}'(n)$ denotes the interfering component at the output of the limiting function, and the ith element of the vector $\mathbf{q}'(n)$ is defined as the following:

$$q_i'(n) = \begin{cases} q_i(n), & \text{if } |\tilde{r}_i(n)| \le \gamma \\ \gamma - \sum_{k=1}^{K} [\mathbf{C}_{k,1}\hat{\mathbf{h}}_k(n)]_i b_k(n), & \text{if } \tilde{r}_i(n) > \gamma \\ -\gamma - \sum_{k=1}^{K} [\mathbf{C}_{k,1}\hat{\mathbf{h}}_k(n)]_i b_k(n), & \text{if } \tilde{r}_i(n) < -\gamma. \end{cases} \tag{48}$$

As mentioned before, the real and imaginary parts of $\tilde{r}_i(n)$ When $\tilde{r}_i(n) > \gamma$, we can observe that $q_i(n) > \gamma - \sum_{k=1}^{K} [\mathbf{C}_{k,1}\hat{\mathbf{h}}_k(n)]_i b_k(n) > 0$, where $[\mathbf{C}_{k,1}\hat{\mathbf{h}}_k(n)]_i$ denotes the ith element of the vector $\mathbf{C}_{k,1}\hat{\mathbf{h}}_k(n)$, and $q_i'(n)$ is further expressed as

$$\begin{aligned} q_i'(n) &= \gamma - \tilde{r}_i(n) + q_i(n) \\ &< q_i(n). \end{aligned} \tag{49}$$

When $\tilde{r}_i(n) < -\gamma$, we observe that $q_i(n) < -\gamma - \sum_{k=1}^{K} [\mathbf{C}_{k,1}\hat{\mathbf{h}}_k(n)]_i b_k(n) < 0$, and $q_i'(n)$ is expressed as

$$q_i'(n) = -\gamma - \tilde{r}_i(n) + q_i(n). \tag{50}$$

Since $q_i(n) < 0$ and $-\gamma - \tilde{r}_i(n) > 0$, we have $|q_i'(n)| < |q_i(n)|$. Concluding from (48)–(50), we can observe that

$$|q_i'(n)| \le |q_i(n)| \tag{51}$$

for all $\tilde{r}_i(n)$. Therefore, the cross-covariance of $q_i'(n)$'s is smaller than that of $q_i(n)$'s, i.e.,

$$|E\{q_i'(n)q_j'(n)^*\}| \le |E\{q_i(n)q_j(n)^*\}| \tag{52}$$

for $i, j = 1, 2, \ldots, N$, where $q_j(n)^*$ denotes the complex conjugate of the interference $q_j(n)$. The inequality in (52) will lead to the improvement of the performance of the proposed adaptive equalization, which will be proved in the next subsection.

B. Analysis of Error Probability

For a sufficiently large N_0, (45) has the following approximation [4]:

$$\begin{aligned} \hat{\mathbf{b}}(n) &\approx \sum_{i=0}^{N_0} \left(\prod_{j=n-i+1}^{n} \mathbf{\Theta}(j) \right) \mathbf{K}_b(n-i) \\ &\quad \times [\mathbf{C}\hat{\mathbf{H}}(n-i)\mathbf{b}(n-i) + \mathbf{q}'(n-i)] \\ &= \mathbf{\Phi}(n)\bar{\mathbf{b}}(n) + \mathbf{\Psi}(n)\bar{\mathbf{q}}'(n) \end{aligned} \tag{53}$$

where we have the equations at the bottom of the page. The symbol estimation of the kth user is given by

$$\tilde{b}_k(n) = \phi_{2k-1}^T(n)\bar{\mathbf{b}}(n) + \psi_{2k-1}^T(n)\bar{\mathbf{q}}'(n) \tag{54}$$

where $\phi_k(n)$ and $\psi_k(n)$ are, respectively, the kth column vector of the matrices $\mathbf{\Phi}^T(n)$ and $\mathbf{\Psi}^T(n)$.

Assuming that the interference $\mathbf{q}'(n)$ is joint Gaussian distributed. The error probability of the kth user is determined by (55), shown at the bottom of the page, where $Q(x) = (1/\sqrt{2\pi}) \int_x^\infty e^{-(t^2/2)} dt$.

Remark 5: When the nonlinear function $\Omega_b(\cdot)$ is applied to the residual $\tilde{\mathbf{r}}(n)$, it will suppress the effect of interference $\mathbf{q}(n)$ and, hence, decrease the amplitude of the entries of the covariance matrix $E\{\bar{\mathbf{q}}'(n)\bar{\mathbf{q}}'(n)^H\}$, whose $(sN+i, tN+j)$ entry is $E\{q_i'(n-s)q_j'(n-t)^*\}$, for $s, t = 0, 1, \ldots, N_0, i, j = 1, 2, \ldots, N$, i.e., $E\{\bar{\mathbf{q}}'(n)\bar{\mathbf{q}}'(n)^H\} \le E\{\bar{\mathbf{q}}(n)\bar{\mathbf{q}}(n)^H\}$ by (52). From (55), it is known that smaller covariance in the denominator of the function $Q(\cdot)$ will reduce the probability of error. This conforms that the proposed robust Kalman method can perform superior to the conventional Kalman filter without the robust algorithm.

$$\begin{aligned} \mathbf{\Theta}(n) &= (\mathbf{I} - \mathbf{K}_b(n)\hat{\mathbf{H}}(n))\mathbf{A} \\ \bar{\mathbf{b}}(n) &= [\mathbf{b}^T(n) \quad \mathbf{b}^T(n-1) \quad \cdots \quad \mathbf{b}^T(n-N_0)]^T \\ \bar{\mathbf{q}}'(n) &= [\mathbf{q}'(n)^T \quad \mathbf{q}'(n-1)^T \quad \cdots \quad \mathbf{q}'(n-N_0)^T]^T \\ \mathbf{\Phi}(n) &= \Bigg[\mathbf{K}_b(n)\mathbf{C}\hat{\mathbf{H}}(n) \quad \mathbf{\Theta}(n)\mathbf{K}_b(n-1)\mathbf{C}\hat{\mathbf{H}}(n-1) \\ &\qquad \cdots \quad \left(\prod_{j=n-N_0+1}^{n} \mathbf{\Theta}(j) \right) \mathbf{K}_b(n-N_0)\mathbf{C}\hat{\mathbf{H}}(n-N_0) \Bigg] \\ \mathbf{\Psi}(n) &= \left[\mathbf{K}_b(n) \quad \mathbf{\Theta}(n)\mathbf{K}_b(n-1) \quad \cdots \quad \left(\prod_{j=n-N_0+1}^{n} \mathbf{\Theta}(j) \right) \mathbf{K}_b(n-N_0) \right]. \end{aligned}$$

$$P_{e,k} = \frac{1}{2^{K(N_0+2)-1}} \sum_{b_k(n)=1, \text{ all } \bar{\mathbf{b}}(n)} Q\left(\frac{\phi_{2k-1}^T(n)\bar{\mathbf{b}}(n)}{\sqrt{\psi_{2k-1}^T(n)E\{\bar{\mathbf{q}}'(n)\bar{\mathbf{q}}'(n)^H\}\psi_{2k-1}(n)}} \right) \tag{55}$$

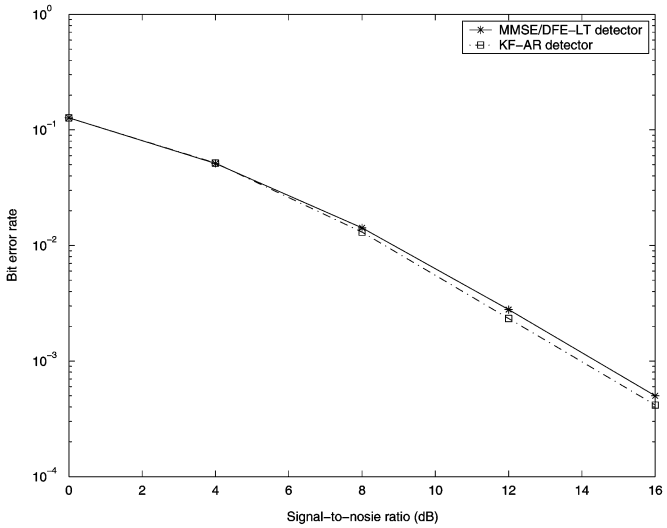

Fig. 9. Bit-error rate of user 1 for the channel with time-varying Doppler frequency.

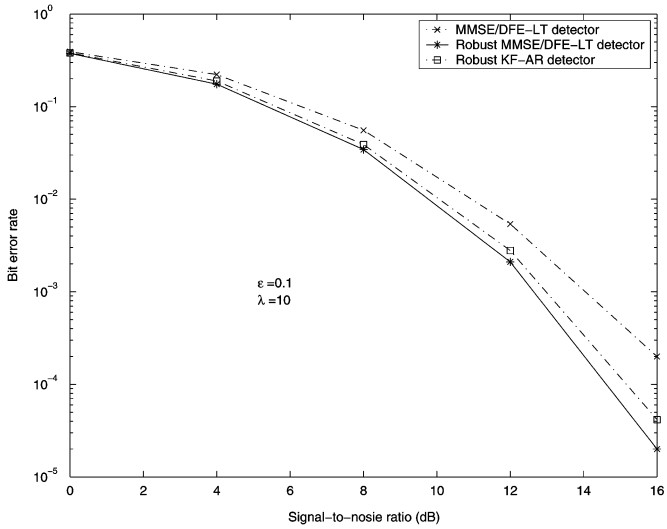

Fig. 10. Bit-error rate of user 1 for the channel with time-varying Doppler frequency disturbed by impulsive noise.

C. Symbol Detection Performance

In the following, we provide some simulation examples to demonstrate the performance gains afforded by the proposed method. The simulation conditions are the same with those we used in Section IV. The time-varying channels simulated in Fig. 6 are employed here. We assume that each user has equal power. The bit-error rate curves of user 1 versus SNR for various multiuser detectors are plotted in Fig. 9. In this example, the ambient noise is normal white Gaussian noise. The proposed MMSE/DFE-LT detector (37)–(40) employs the channel estimates obtained from (23) via the LT model. The KR–AR detector employs the conventional Kalman filter [20] for symbol detection based on the channel estimates via the AR(2) model. It is seen that the proposed detector based on the LT channel model, without the knowledge of exact Doppler frequency, performs very close to that of the AR(2) model-based symbol detector with the knowledge of exact Doppler frequency.

Fig. 10 gives the BER performances for these detection methods over impulsive noise. The non-Gaussian noise is generated by the two-term Gaussian mixture model depicted in (31) with parameters $\varepsilon = 0.1, \lambda = 10$. The threshold γ in (43) of the limiting function $\Omega_x(\cdot)$ is defined according to the estimated channel parameters, as indicated in (44). The proposed robust MMSE/DFE-LT detector in (45) is implemented based on the channel estimates obtained from the robust channel estimator (29) via the LT model, whereas the robust KR–AR detector performs symbol detection similar to (45). However, the sign function is excluded. The results show that the robust estimators (with the aid of the limiting function $\Omega_x(\cdot)$, which can suppress the impulse-like noise) achieve better performance than the estimators without the limiting function. In the presence of impulse noise, signal samples may be contaminated with strong impulses, resulting in unreliable decision output. In this situation, the robust MMSE/DFE-LT detector and the robust KR-AR detector, which are embedded with limitation functions $\Omega_x(\cdot)$, can provide robust BER performances.

VI. Conclusion

In this paper, a robust linear-trend (LT) channel estimation algorithm and a robust multiuser detection algorithm are combined for DS/CDMA communication systems over multipath time-varying fading channel with impulsive noise. Both of them employ the robust Kalman state estimator with a nonlinear limiting function to enhance their performances. A self-tuning scheme to automatically adjust the variance of the driving noise in the state-space model is proposed to cope with the time-varying Doppler frequency. A robust Kalman-based DFE detection algorithm based on the estimated channel impulse response is also proposed to prevent severe error propagation due to impulsive noise and channel estimation error under time-varying fading channels and impulsive noise. In contrast to the autoregressive (AR) model, since the parameters of the LT channel model do not need actual Doppler frequency to modify the model coefficients, it has the advantage of practical applications. Simulation results indicate that the proposed method outperforms the conventional detectors in a frequency-selective Rayleigh fading channel. The reason is that the proposed Kalman-based DFE method is more robust in channel estimation and symbol detection via the use of LT channel model, hard decision feedback, and nonlinear limiting function in the detection algorithm of the DS/CDMA communications.

References

[1] K. S. Gilhousen, I. M. Jacobs, R. Padovani, A. J. Viterbi, L. A. Weaver Jr., and C. E. Wheatley III, "On the capacity of a cellular CDMA system," *IEEE Trans. Veh. Technol.*, vol. 40, no. 2, pp. 303–312, May 1991.

[2] S. Verdu, "Minimum probability of error for asynchronous Gaussian multiple access channels," *IEEE Trans. Inf. Theory*, vol. IT-32, no. 1, pp. 85–96, Jan. 1986.

[3] T. J. Lim, L. K. Rasmussen, and H. Sugimoto, "An asynchronous multiuser CDMA detector based on the Kalman filter," *IEEE J. Sel. Areas Commun.*, vol. 16, no. 9, pp. 1711–1722, Dec. 1998.

[4] T. J. Lim and Y. Ma, "The Kalman filter as the optimal linear minimum mean-squared error multiuser CDMA detector," *IEEE Trans. Inf. Theory*, vol. 46, no. 7, pp. 2561–2566, Nov. 2000.

[5] H. Y. Wu and A. Duel-Hallen, "Multiuser detectors with disjoint Kalman channel estimators for synchronous CDMA mobile radio channels," *IEEE Trans. Commun.*, vol. 48, no. 5, pp. 752–756, May 2000.
[6] C. Xiao, Y. R. Zheng, and N. C. Beaulieu, "Second-order statistical properties of the WSS Jakes' fading channel simulator," *IEEE Trans. Commun.*, vol. 50, no. 6, pp. 888–891, June 2002.
[7] R. A. Iltis, "A tracking mode receiver for joint channel estimation and detection of asynchronous CDMA signals," in *Conf. Rec. Thirty-Third Asilomar Conf. Signals, Syst., Comput.*, vol. 2, 1999, pp. 998–1002.
[8] B. C. W. Lo and K. B. Letaief, "Adaptive equalization and interference cancellation for wireless communication systems," *IEEE Trans. Commun.*, vol. 47, no. 4, pp. 538–545, Apr. 1999.
[9] H. V. Poor and X. Wang, "Code-aided interference suppression for DS/CDMA communications, Part I: Interference suppression capability, Part II: Parallel blind adaptive implementations," *IEEE Trans. Commun.*, vol. 45, pp. 1101–1122, Sep. 1997.
[10] R. Fantacci, S. Morosi, and M. Bonechi, "Adaptive MMSE receivers for communications in nonstationary multipath fading channel," in *Proc. IEEE Sixth Int. Symp. Spread Spectrum Techn. Applications*, vol. 2, 2000, pp. 545–549.
[11] S. Verdu, *Multiuser Detection*. Cambridge, U.K.: Cambridge Univ. Press, 1998.
[12] D. Divsalar and M. K. Simon, "Improved parallel interference cancellation for CDMA," *IEEE Trans. Commun.*, vol. 46, no. 2, pp. 258–268, Feb. 1998.
[13] S. Tsai, T. F. Wong, and J. S. Lehnert, "Joint channel estimation and MAP detection in time-selective CDMA channels," in *Proc. Wireless Commun. Networking Conf.*, vol. 3, 1999, pp. 1484–1488.
[14] A. M. Sayeed and B. Aazhang, "Joint multipath-Doppler diversity in mobile wireless communications," *IEEE Trans. Commun.*, vol. 47, no. 1, pp. 123–132, Jan. 1999.
[15] X. Wang and H. V. Poor, "Robust multiuser detection in non-Gaussian channels," *IEEE Trans. Signal Process.*, vol. 47, no. 2, pp. 289–305, Feb. 1999.
[16] W. R. Wu and A. Kandu, "Recursive filtering with non-Gaussian noise," *IEEE Trans. Signal Process.*, vol. 44, no. 6, pp. 1454–1468, Jun. 1996.
[17] X. Wang and H. V. Poor, "Blind equalization and multiuser detection in dispersive CDMA channels," *IEEE Trans. Commun.*, vol. 46, no. 1, pp. 91–103, Jan. 1998.
[18] B. S. Chen and T. Y. Dong, "Robust stability analysis of Kalman filter under parametric and noise uncertainties," *Int.. J. Contr.*, vol. 48, no. 6, pp. 2189–2199, 1988.
[19] P. J. Brockwell and R. A. Davis, *Time Series: Theory and Methods*, Second ed. New York: Spring-Verlag, 1991.
[20] S. Haykin, *Adaptive Filter Theory*. Englewood Cliffs, NJ: Prentice-Hall, 1996.
[21] W. C. Jakes, *Microwave Mobile Communications*. Piscataway, NJ: IEEE Press, 1974.
[22] P. J. Huber, *Robust Statistics*. New York: Wiley, 1981.

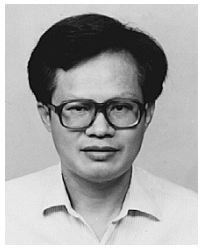

Bor-Sen Chen (M'82–SM'89–F'01) received the B.S. degree from Tatung Institute of Technology, Taipei, Taiwan, R.O.C., the M.S. degree from National Central University, Chungli, Taiwan, and the Ph.D degree from the University of Southern California, Los Angeles, in 1970, 1973 and 1982, respectively.

He was a Lecturer, Associate Professor, and Professor at the Tatung Institute of Technology from 1973 to 1987. He is currently a Tsing Hua Professor of electrical engineering and computer science at National Tsing Hua University, Hsinchu, Taiwan. His current research interests are in control engineering, signal processing and system biology. He is a member of the Editorial Advisory Board of two journals (the *International Journal of Fuzzy Systems* and the *International Journal of Control, Automation and Systems*) and editor of the *Asian Journal of Control*.

Dr. Chen has received the Distinguished Research Award from National Science Council of Taiwan four times. He is a Research Fellow of the National Science Council of Taiwan and holds the excellent scholar Chair in engineering. He has also received the Automatic Control medal from the Automatic Control Society of Taiwan in 2001. He is an associate editor of IEEE TRANSACTIONS ON FUZZY SYSTEMS He is a Fuzzy Systems Technical Committee member of the IEEE Neural Network Council.

Chang-Lan Tsai received the B.S. degree in electrical engineering from National Chung Hsing University, Taichung, Taiwan, R.O.C., in 1996 and the M.S. degree in electrical engineering from National Tsing Hua University, Hsinchu, Taiwan, in 1998. He is currently working toward the Ph.D. degree in electrical engineering at National Tsing Hua University.

His current research interests include equalization problems in multiuser communication systems.

Chia-Sheng Hsu was born in Taiwan, R.O.C., in 1977. He received the B.S. degree in communication engineering from National Chiao Tung University, Hsinchu, Taiwan, in 1999 and the M.S. degree in electrical engineering from National Tsing Hua University, Hsinchu, Taiwan, in 2001.

Currently, he is a firmware engineer with the Department of Algorithm Development, Sunplus Technology Co., Ltd., Hsinchu. His research interests include wireless communication, speech signal processing, DSP and VLSI applications, and multimedia signal processing.